L-selectin-mediated leukocyte tethering in shear flow is controlled by multiple contacts and cytoskeletal anchorage facilitating fast rebinding events

Ulrich S. Schwarz*† and Ronen Alon‡

*Theory Division, Max Planck Institute of Colloids and Interfaces, 14424 Potsdam, Germany; and ‡Department of Immunology, Weizmann Institute of Science, Rehovot 76100, Israel

Edited by Robert Langer, Massachusetts Institute of Technology, Cambridge, MA, and approved March 16, 2004 (received for review September 11, 2003)

L-selectin-mediated tethers result in leukocyte rolling only above a threshold in shear. Here we present biophysical modeling based on recently published data from flow chamber experiments, which supports the interpretation that L-selectin-mediated tethers below the shear threshold correspond to single L-selectin carbohydrate bonds dissociating on the time scale of milliseconds, whereas L-selectin-mediated tethers above the shear threshold are stabilized by multiple bonds and fast rebinding of broken bonds, resulting in tether lifetimes on the time scale of 10^{-1} seconds. Our calculations for cluster dissociation suggest that the single molecule rebinding rate is of the order of 10^4 Hz. A similar estimate results if increased tether dissociation for tail-truncated L-selectin mutants above the shear threshold is modeled as diffusive escape of single receptors from the rebinding region due to increased mobility. Using computer simulations, we show that our model yields first-order dissociation kinetics and exponential dependence of tether dissociation rates on shear stress. Our results suggest that multiple contacts, cytoskeletal anchorage of L-selectin, and local rebinding of ligand play important roles in L-selectin tether stabilization and progression of tethers into persistent rolling on endothelial surfaces.

Leukocyte trafficking plays a central role in the immune response of vertebrates. Leukocytes constantly circulate in the cardiovascular system and enter into tissue and lymph through a multistep process involving rolling on the endothelium, activation by chemokines, arrest, and transendothelial migration (1). A key molecule in this process is L-selectin, a leukocyte-expressed adhesion receptor that is localized to tips of microvilli and binds to glycosylated ligands on the endothelium. Its properties are optimized for initial capture and rolling under physiological shear (2, 3), as confirmed by recent experimental data and computer simulations (4, 5). In contrast to tethering through other receptor systems like P-selectin, E-selectin, or integrins, appreciable tethering through L-selectin and subsequent rolling occurs only above a threshold in shear (6), even in cell-free systems (7, 8). Down-regulation by low shear is unique for L-selectin tethers and might be necessary because L-selectin ligands are constitutively expressed on circulating leukocytes, platelets, and subsets of blood vessels (9).

The dissociation rate of single molecular bonds is expected to depend exponentially on an externally applied steady force (Bell equation) (10). Quantitative analysis with a regular video camera (time resolution of 30 ms) of L-selectin tether kinetics in flow chambers above the shear threshold resulted in first-order dissociation kinetics, with a force dependence that could be fit well to the Bell equation, resulting in a force-free dissociation constant of 6.6 Hz (2–4, 11). These findings have been interpreted as signatures of single L-selectin carbohydrate bonds. However, recent experimental evidence suggests that L-selectin tether stabilization involves multiple bonds and local rebinding events. Evans *et al*. (12) used the biomembrane force probe to measure unbinding rates for single L-selectin bonds as a function of loading force (12). Modeling bond rupture as thermally activated escape over a sequence of transition state barriers increasingly lowered by rising force (13), these experiments revealed two energy barriers along the unbinding pathway. The inner barrier corresponds to Ca^{2+}-dependent binding through the lectin domain and explains the high strength of L-selectin-mediated tethers required for cell capture from shear flow. Extracting barrier properties from dynamic force spectroscopy data allows their conversion into a plot of dissociation rate as a function of force. In this way, results from dynamic force spectroscopy and flow chamber experiments can be compared independently of loading rate. In detail, Evans *et al*. (12) found a 1,000-fold increase in dissociation rate as force rises from 0 to 200 pN, in marked contrast to tether dissociation kinetics as measured in flow chamber experiments, which increases at most 10-fold over this range (2, 3). Therefore, additional stabilization has to be involved with leukocyte tethers mediated by L-selectin.

Dwir *et al*. (14) used flow chambers to study tethering of leukocytes transfected with tail-modified mutants of L-selectin. They found that tether dissociation increases with increased tail truncation, possibly because tail truncation leads to decreased cytoskeletal anchorage and increased mobility. More recently, Dwir *et al*. (15) found with a high-speed video camera (time resolution of 2 ms) that L-selectin tethers form even below the shear threshold at shear rate 40 Hz, albeit with a very fast dissociation rate of 250 Hz, undetectable with a regular camera. Thus the shear threshold results from insufficient tether stabilization at low shear. Using systematic changes in viscosity (which changes shear stress but not shear rate), Dwir *et al*. (15) were able to show that at the shear threshold, tether lifetime is prolonged by a factor of 14 due to shear-mediated cell transport over L-selectin ligand. They suggested that sufficient transport might be needed for formation of additional bonds. With more than one bond present, rebinding could then provide the tether stabilization observed experimentally.

In this paper, we present a theoretical model for the interplay between bond rupture, L-selectin mobility, and ligand rebinding within small clusters of L-selectin bonds, which interprets recent experimental results in a consistent and quantitative way. Traditionally, tether dissociation at low ligand density has been interpreted as single-molecule rupture due to observed first-order dissociation kinetics and a shear dependence that can be fit well to the Bell equation. Here we demonstrate that the same features result for small clusters of multiple bonds with fast rebinding. Our results suggest that the shear threshold corresponds to the formation of multiple contacts, and that single L-selectin bonds decay too rapidly to provide functional leukocyte tethers.

This paper was submitted directly (Track II) to the PNAS office.

†To whom correspondence should be addressed. E-mail: ulrich.schwarz@mpikg-golm.mpg.de.

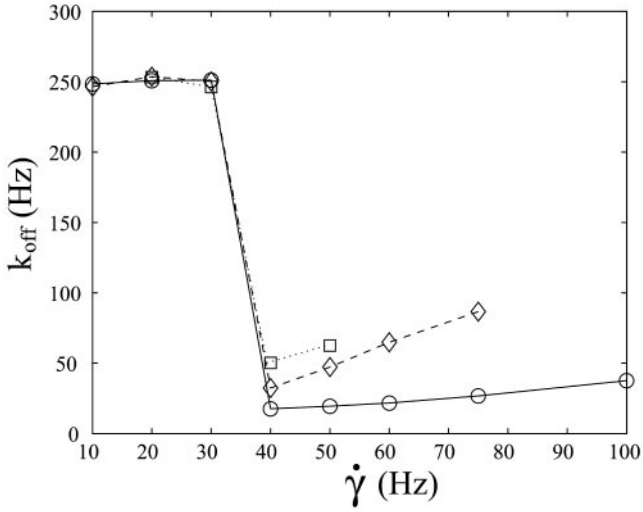

Fig. 1. Tether dissociation rate k_{off} determined from kinetic analysis of flow chamber experiments plotted as function of shear rate $\dot{\gamma}$ (15). Solid line with circles: wild type. Dashed line with diamonds: tail-deleted mutant. Dotted line with squares: wild type with 6% of Ficoll, which changes viscosity and thus shear stress (but not shear rate) by a factor of 2.6. These data suggest that the shear threshold is a transport- rather than a force-related issue, and that the shear threshold is not about ligand recognition but about tether stabilization.

Experiments

Our experimental procedures have been described elsewhere (14, 15). Three variants of human L-selectin were stably expressed in the mouse 300.19 pre B cell line. Wild-type, tail-truncated and tail-deleted mutants have the same extracellular domains and differ only in their cytoplasmic tails. L-selectin-mediated tethering was investigated in a parallel plate flow chamber. The main ligand used was PNAd, the major L-selectin glycoprotein ligand expressed on endothelium. For immobilization in the flow chamber, the ligand was diluted so that no rolling was supported at shear rates lower than 100 Hz (dilution 10 ng/ml in the coating solution, which corresponds to an approximate scaffold density of $100/\mu m^2$). Single tethers were monitored with video microscopy at 2-ms resolution, and the microkinetics were analyzed by single cell tracking, as described (14, 15). The logarithm of the number of cells that pause longer than time t is plotted as a function of t and usually gives a straight line indicative of an effectively first-order dissociation process. The slope is the tether dissociation rate k_{off} and is plotted as a function of shear rate $\dot{\gamma}$ in Fig. 1. This plot shows that below the shear threshold of 40 Hz, the dissociation rate is 250 Hz, independent of tail mutations and viscosity of the medium. Above the shear threshold, the dissociation rate becomes force-dependent, with a dependence on shear stress that can be fit well to the Bell equation $k_{off} = k_0 e^{F/F_b}$ (10). Here k_0 is the force-free dissociation rate, and F_b is the bond's internal force scale. The force on an undeformed 300.19 lymphocyte with radius $R = 6$ μm follows from Stokes flow around a sphere close to a wall (16). Taking into account the lever arm geometry provided by the tether holding the cell at an angle of 50°, the force acting on the L-selectin bonds can be calculated to be $F = 180$ pN per dyn/cm^2 of shear stress (3). Fitting the Bell equation to the wild-type data from Fig. 1 gives values similar to those obtained in earlier studies (2–4, 11), namely a force-free dissociation constant of 6.6 Hz and an internal force scale $F_b = 200$ pN (corresponding to a reactive compliance of 0.2 Å). At the shear threshold, we find 14- and 7-fold reduction in dissociation rate for wild-type and tail-truncated mutant, respectively. Adding 6 volume percent of the nontoxic sugar Ficoll increases viscosity from 1 cP to 2.6 centipoise (cP; 1 P = 0.1 Pa·sec). Thus shear stress is increased by a factor of 2.6, whereas shear rate is unchanged. At the shear threshold, this increases wild-type dissociation 3-fold, roughly as expected from the fit to the Bell equation. Most importantly, there is no shift of the shear threshold as a function of shear rate. This indicates that the shear threshold results from shear-mediated transport, rather than from a force-dependent process.

Theory

Shear-Mediated Transport. At the shear threshold at shear rate $\dot{\gamma} = 40$ Hz (corresponding to shear stress $\tau = \eta\dot{\gamma} = 0.4$ dyn/cm^2 for viscosity $\eta = 1$ cP) and for small distance between cell and substrate, a cell with radius $R = 6$ μm will translate with hydrodynamic velocity $u = 0.48\, R\dot{\gamma} = 0.12$ μm/ms and at the same time rotate with frequency $\Omega = 0.26\ \dot{\gamma} = 10.4$ Hz (16). Therefore the cell surface and the substrate surface will move relatively to each other with an effective velocity $v = u - R\Omega = 0.22\, R\dot{\gamma} = 50$ nm/ms. In average, there is no normal force that pushes the cell onto the substrate, but because it moves in close vicinity to the substrate, it can explore it with this effective velocity v. Thus there exists a finite probability for a chance encounter between L-selectin receptors on the tip of a microvillus and a carbohydrate ligand on the substrate. Here we focus on the case of diluted ligands, with a ligand density of $100/\mu m^2$. Then the average distance between single ligands is 100 nm, larger than the lateral extension of the microvilli, which is 80 nm. Therefore the first tethering event is very likely to be a single molecular bond (Fig. 2*a*). If this first bond has formed, the microvillus will be pulled straight, and the cell will slow down. It will come to a stop on the distance x of order μm (e.g., the rest length of a microvillus is 0.35 μm). This takes the typical time $t_s = x/u = 8$ ms. During this time, the cell can explore an additional distance of the order of $vt_s = 400$ nm. The experimental data presented in Fig. 1 suggest that this is the minimal transport required to establish a second microvillar contact able to contribute to tether stabilization (Fig. 2*b*).

Single Bond Loading. If tether duration was much longer than the time over which the cell comes to a stop, the single bond dissociation rate k_{off} below the shear threshold should increase exponentially with shear rate $\dot{\gamma}$ according to the Bell equation. However, this assumption is not valid in our case, because tether duration and slowing down time are both in the millisecond range. Fig. 3 shows that indeed the Bell equation (dotted line) does not describe the wild-type data from Fig. 1 (dashed line with circles). To model a realistic loading protocol, we assume that the force on the bond rises linear until time t_s and then plateaus at the constant force F arising from shear flow. Note that initial loading rate $r = F/t_s$ scales quadratically with shear rate $\dot{\gamma}$, because $F \approx \dot{\gamma}$ and $t_s \approx 1/\dot{\gamma}$. The dissociation rate k_{off} for this situation can be calculated exactly. The result is given in *Supporting Text*, which is published as supporting information on the PNAS web site and is plotted as dash-dotted line in Fig. 3. It is considerably reduced toward the experimentally observed plateau. Agreement is expected to increase further if initial loading is assumed to be sublinear. A scaling argument shows the main mechanism at work. For the case of pure linear loading, the mean time to rupture is $T = (F_b/r)\exp(k_0 F_b/r)\, E(k_0 F_b/r)$, where $E(x)$ is the exponential integral (17). There are two different scaling regimes for slow and fast loading, which are separated by the critical loading rate $r_c = k_0 F_b$. For slow loading, $r < r_c$, a large argument expansion gives $T \approx 1/k_0$, that is the bond decays by itself before it starts to feel the effect of force. For fast loading, a small argument expansion gives $T \approx (F_b/r)\ \ln\,(r/k_0 F_b)$, which is also found for the most frequent time of rupture in this regime (13). In our case, $k_0 = 250$ Hz, $F_b = 200$ pN, and $r_c = k_0 F_b = 5 \times 10^4$ pN/s. At the shear threshold, $r = 10^4$ pN/s, and we are still in the regime of slow loading, $r < r_c$. This suggests that tethers

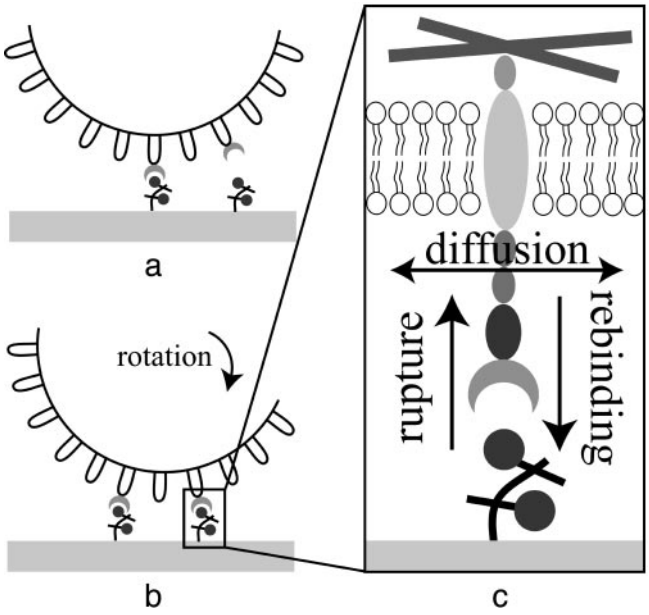

Fig. 2. A schematic representation of the mechanisms involved in L-selectin-mediated leukocyte tethering to diluted carbohydrate ligands. (*a*) Initial binding most likely corresponds to one L-selectin receptor localized to the tip of one microvillus binding to ligand presented on a glycoprotein scaffold on the substrate. At low shear, stabilization through additional bonds is unlikely, because the distance between scaffolds is larger than the microvilli's tips, and the probability of two microvilli simultaneously hitting two ligands is very low. (*b*) At sufficiently high shear, shear-mediated rotation of the cell over the substrate leads to the establishment of an additional bond on another microvillus. In contrast to this 2D cartoon, in practice, the two microvilli are expected to coexist with similar latitude, so they can share force in a cooperative way. (*c*) Close-up of the cell–substrate interface. The L-selectin receptor can move laterally in the membrane, with an effective diffusion constant that depends on cytoskeletal anchorage. If a receptor has bound to ligand on the substrate, it will rupture in a stochastic manner, depending on shear-induced loading. If an additional bond (most likely on the second microvillus) holds the cell during times of rupture, rebinding can occur at the first microvillus, thus increasing tether stabilization.

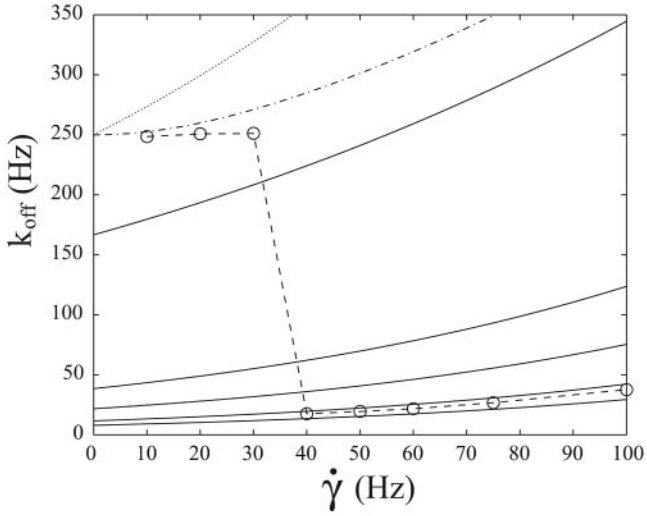

Fig. 3. Theoretical predictions for tether dissociation rate k_{off} as a function of shear rate $\dot{\gamma}$ compared to experimentally measured wild-type data from Fig. 1 (dashed line with circles). Dotted line: the single-bond dissociation rate with force-free dissociation rate $k_0 = 250$ Hz and constant instantaneous loading increases exponentially according to the Bell equation. Dash-dotted line: it is reduced toward the experimentally observed plateau below the shear threshold at $\dot{\gamma} = 40$ Hz by including the effect of finite loading rates. Solid lines from top to bottom: cluster dissociation rate for two-bonded tether with rebinding rate $k_{on} = 0$, 10, 20, 40, and 60 k_0. Above the shear threshold, the two-bonded tether with $k_{on} \approx 10^4$ Hz agrees well with the experimentally measured data.

below the shear threshold correspond to single L-selectin carbohydrate bonds, which decay before the effect of force becomes appreciable. This does not imply that the bonds do not feel any force (after all of the cell is slowed down), but that we are in a regime in which k_{off} as a function of shear does not change appreciably, as observed experimentally.

Single Bond Rebinding. Single bond rupture is a stochastic process according to the dissociation rate k_{off} given by the Bell equation. If ligand and receptor remain in spatial proximity after rupture, rebinding becomes possible. We define the single molecule rebinding rate k_{on} to be the rate for bond formation when receptor and ligand are in close proximity. If bond formation was decomposed into transport-determined formation of an encounter complex and chemical reaction of the two partners, then k_{on} would correspond to the on-rate for reaction (10, 18). It has the dimension of 1/s and should not be confused with 2D or 3D association rates, which have dimensions of m^2/s (equivalently m/Ms) and m^3/s (equivalently 1/Ms), respectively. k_{on} should depend mainly on the extracellular side of the receptor. In the following, it will therefore be assumed to be the same for wild-type and mutants. There are two mechanisms that might prevent rebinding within an initially formed cluster: the single receptor might escape from the rebinding region due to lateral mobility, or the receptor might be carried away from the ligand because the cell is carried away by shear flow. Fig. 2*c* shows schematically the interplay between rupture, rebinding, and mobility for single L-selectin receptors.

We start with the first case, diminished rebinding due to lateral receptor mobility. Because increased tail truncation decreases interaction with the cytoskeleton (19), lateral mobility increases from wild-type through tail-truncated to tail-deleted mutant. For each receptor type, we assume an effective diffusion constant D. The conditional probability for rebinding depends on absolute time since rupture. We approximate it by the probability that a particle with 2D diffusion but without capture is still within a disk with capture radius s at time t, $k_{on}(t) = k_{on}(1 - e^{-s^2/4Dt})$. Thus the time scale for the diffusion correction is set by $s^2/4D$, the time to diffuse the distance of the capture radius. The diffusion constant for the wild type can be estimated to be 10^{-11} cm^2/s, with the one for the tail-deleted mutant being at least one order of magnitude larger (20, 21). A typical value for the capture radius is s = 1 nm. Then the time $t_c = s^2/4D$ to diffuse this distance is 250 and 25 μs for wild-type and tail-deleted mutant, respectively. For smaller times, $t < t_c$, k_{on} plateaus at its initial value. For larger times, $t > t_c$, it decays rapidly toward zero. The single molecule behavior is governed by the dimensionless number $k = k_{on}\, s^2/4D$, which is the ratio of time scales set by diffusion and rebinding. Diffusion does not interfere with rebinding as long as $k > 1$. Our theory therefore predicts that for wild-type with diffusion constant $D = 10^{-11}$ cm^2/s and capture radius s = 1 nm, $k_{on} > 4 \times 10^3$ Hz. For the tail-deleted mutant, mobility does interfere with rebinding, and we must have $k < 1$. If we assume that in this case D is smaller by one order of magnitude, then $k_{on} < 4 \times 10^4$ Hz. Thus we can conclude that k_{on} should be of the order of 10^4 Hz.

Tether Stabilization Through Multiple Bonds. We now turn to the possibility that spatial proximity required for rebinding is established by multiple contacts. Tethers above the shear threshold are modeled as clusters of N bonds, which in practice are expected to be distributed over at least two microvilli. At any time point, each of the N bonds is either closed or open. The way

force is shared between the closed bonds depends on the details of each tether realization. However, we expect that only those realizations will contribute significantly to the long-lived tethers above the shear threshold in which different bonds share force more or less equally. This most likely corresponds to two microvilli being bound with similar latitude in regard to the direction of shear flow. With this assumption, the force used in the single molecule dissociation rate has to be overall force divided by the number of closed bonds. If one bond ruptures, force is redistributed among the remaining bonds. Open bonds can rebind with the rebinding rate k_{on}. If rebinding occurs, force again is redistributed among the closed bonds. In general, in the absence of diffusion cluster lifetime T, but not the full cluster dissociation probability function can be calculated exactly (22). We first discuss the case without loading or diffusion, thus focusing on the role of rebinding. As argued in *Supporting Text*, for small rebinding rate, $k_{on} < k_0$, cluster lifetime T scales logarithmically rather than linear with cluster size N. This weak increase in T with N results because different bonds decay not one after the other, but on the same time scale. The exact treatment shows that for clusters of 2, 10, 100, 1,000, and 10,000 bonds without rebinding, lifetime is prolonged by 1.5, 2.9, 5.2, 7.5, and 9.8, respectively. To achieve 14-fold stabilization as observed experimentally at the shear threshold, one needs the astronomical number of 6×10^5 bonds. In practice, for the case of dilute ligand discussed here, only very few bonds are likely. Therefore even in the presence of multiple bonds, rebinding is essential to provide tether stabilization.

In general, fast rebinding is much more efficient for tether stabilization than large cluster size. Our calculations predict that, to obtain 14-fold stabilization for the cases $N = 2$, 3, and 4, one needs $k_{on} = 6 \times 10^3$, 10^3 and 550 Hz, respectively. The value $k_{on} = 6 \times 10^3$ Hz obtained for the case $N = 2$ is surprisingly close to the estimate $k_{on} = 10^4$ Hz obtained above via a completely different route, namely the competition of rebinding and diffusion for a single molecule. Therefore in the following, we restrict ourselves to the simple case of two bonds being formed above the shear threshold (most probably by two microvilli). In this case, cluster lifetime can be calculated to be (22):

$$T = \frac{1}{2k_0}\left(e^{-F/2F_b} + 2e^{-F/F_b} + \frac{k_{on}}{k_0}e^{-3F/2F_b}\right) \qquad [1]$$

A derivation of this result is given in *Supporting Text*. In Fig. 3, we use Eq. **1** to plot the dissociation rate for the two-bonded tether (identified with the inverse of cluster lifetime T) as a function of shear rate for different values of rebinding. The shear threshold at 40 Hz corresponds to $F = 0.36\,F_b$. It follows from Eq. **1** that for this value of F, 14-fold stabilization in comparison with the force-free single bond lifetime is achieved for $k_{on} \approx 44\ k_0$. For $k_0 = 250$ Hz, this corresponds to a rebinding rate of $k_{on} = 1.1 \times 10^4$ Hz. Thus again we arrive at the same order of magnitude estimate, $k_{on} = 10^4$ Hz. Fig. 3 shows that with this value for k_{on}, agreement between theory and experimental wild-type data above the shear threshold is surprisingly good.

Relation to BIAcore. We now discuss how our estimate relates to BIAcore (Piscataway, NJ) data for L-selectin (23). In this experiment, L-selectin was free in solution and GlyCAM-1 immobilized on the sensor surface, which makes it a monovalent ligand. For the equilibrium dissociation constant, the authors (23) found $K_d = 105\ \mu$M. This unusually low affinity results from a very large dissociation rate k_r, which they estimated to be $k_r \gtrsim 10$ Hz. The results presented in Fig. 1 seem to suggest that the real dissociation rate $k_r = 250$ Hz. However, surface anchorage of both counterreceptors often reduces bond lifetime by up to two orders of magnitude (24). This has been demonstrated

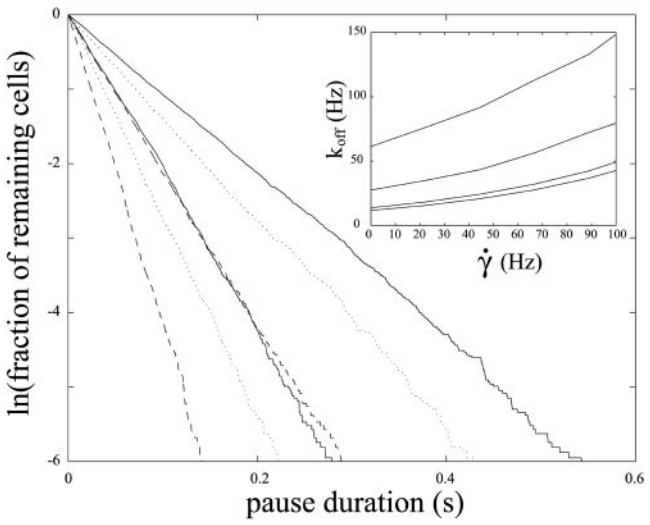

Fig. 4. Computer simulations show that L-selectin-mediated tethers above the shear threshold yield first-order dissociation kinetics. Solid lines: two-bonded tether with $F = 0$ and $k_{on} = 10^4$ (*Right*) and 0.5×10^4 Hz (*Left*). Dashed lines: the same with $F = 100$ pN. Dotted lines: $k_{on} = 10^4$, $F = 0$, and mobility parameter $k = k_{on}\,s^2/4D = 1$ (*Right*) and 0.5 (*Left*), respectively. (*Inset*) L-selectin-mediated tethers show Bell-like shear dependence even in the presence of L-selectin mobility. Solid lines from bottom to top: no mobility, $k =$ 2.5, 1, and 0.5.

experimentally for several receptor–ligand systems and might result from the reduction in free enthalpy of the anchored bond. Thus it might well be that the dissociation rate $k_0 = 250$ Hz found for surface anchored bonds might be reduced down to $k_r = 10$ Hz for free L-selectin binding to surface-bound ligand. Then the association rate $k_f = 10^5$ 1/Ms. For a capture radius s = 1 nm and a 3D diffusion constant $D = 10^{-6}$ cm^2/s, the diffusive forward rate in solution is $k_+ = 4\pi D\,s = 8 \times 10^8$ 1/Ms. Because $k_+ > k_f$, the receptor–ligand binding in solution is reaction-limited, as it usually is. As explained above, k_{on} can be identified with the rate with which an encounter complex transforms into the final product (10, 18). Because bond formation is reaction-limited, $k_{on} = k_f K_+ = 4 \times 10^4$ Hz, where $K_+ = 3/4\ \pi s^3$ is the dissociation constant of diffusion. Thus this estimate agrees well with the two other estimates derived above.

Computer Simulations. To obtain effective dissociation rates in the presence of diffusion, one has to use computer simulations. For each parameter set of interest, we used Monte Carlo simulations to simulate 5,000 realizations according to the rates given above. More details are described in the *Supporting Text*. In general, our simulations show that for strong rebinding, that is $k_{on} > k_0$, the effective dissociation kinetics of small clusters is first order. In Fig. 4, this is demonstrated for the case $N = 2$. The plot shows the logarithm of the simulated number of tethers lasting longer than time t for different parameter values of interest. All curves are linear, even in the presence of mobility, and the slopes can be identified with the dissociation rates. For example, $k_{on} = 10^4$ Hz and $F = 100$ pN yields the same effective first order dissociation rate as $k_{on} = 0.5 \times 10^4$ Hz and $F = 0$, thus rebinding can rescue the effect of force. Our simulations also show that cluster dissociation rate as a function of force fits well to the Bell equation for $k_{on} > k_0$. In particular, this holds true in the presence of L-selectin mobility, as shown in Fig. 4 *Inset*. For $k_{on} = 10^4$ Hz and without mobility (vanishing diffusion constant), lifetime at the shear threshold is 12-fold increased compared with single bond dissociation. With our estimate for wild-type mobility ($k = k_{on}$

$s^2/4D = 2.5$), 10-fold stabilization takes place. For tail-deleted mobility ($k = 0.25$), only 1.5-fold stabilization occurs. This effect is more dramatic than observed experimentally, where stabilizations for wild-type and tail-deleted mutants are 14- and 7-fold, respectively. In practice, the mobility scenario is certainly more complicated and is expected to smooth out the threshold effect arising from our modeling.

Discussion

In this paper, we have presented biophysical modeling of L-selectin tether stabilization in shear flow based on recently published flow chamber data with high temporal resolution (15). Our analysis suggests that the 14-fold stabilization observed at the shear threshold results from formation of multiple contacts and a single molecule rebinding rate of the order of $k_{on} = 10^4$ Hz, which is remarkably faster than the force-independent dissociation rate $k_0 = 250$ Hz observed below the shear threshold. Using computer simulations, we showed that for such strong rebinding, the experimentally observed first-order dissociation and Bell-like shear force dependence follow from the statistics of small clusters of bonds. Despite the good quantitative agreement achieved here between experimental data and our model, it is important to state that it cannot be expected to predict all details of the experimental results. In practice, the formation of bonds is a stochastic process, and there will be a statistical mixture of differently sized and differently loaded clusters, involving different microvilli and different scaffolds of L-selectin ligands. Cytoskeletal anchorage of the different ligand-occupied L-selectin molecules might also change in time in a complex way. Nevertheless, by focusing on the case of two bonds (possibly on two different microvilli) with shared loading and mobility-dependent rebinding, we obtained quantitative explanations for many conflicting observations from flow chamber experiments and biomembrane force probes, which have not been interpreted in a consistent way before.

Several explanations have been proposed for the shear threshold effect. Chang and Hammer (25) suggested that faster transport leads to increased probability for receptor ligand encounter. Yet the new high-resolution data from flow chamber experiments indicate that below the shear threshold, the issue is insufficient stabilization rather than insufficient ligand recognition (15). Chen and Springer (4) suggested that increased shear helps to overcome a repulsive barrier, possibly resulting from negative charges on the mucin-like L-selectin ligands. However, Dwir *et al.* (15) showed that small oligopeptide ligands for L-selectin presented on nonmucin avidin scaffolds exhibit the same shear dependence as their mucin counterparts. Evans *et al.* (12) have argued that increased shear leads to cell flattening and bond formation. However, Dwir *et al.* (15) found that fixation of PSGL-1-presenting neutrophils does not change the properties of tethers formed on low-density immobilized L-selectin, whereas they do destabilize PSGL-1 tethers to immobilized P-selectin (O. Dwir and R.A., unpublished data). These data suggest that cell deformation, as well as stretching and bending of microvilli, does not play any significant role in L-selectin tether stabilization. Recently, the unusual molecular property of catch bonding has been suggested as an explanation for the shear threshold (26, 27). However, the data by Dwir *et al.* (15) suggest that force-related processes do not account for the shear threshold of L-selectin-mediated tethering. Our interpretation of the shear threshold as resulting from multiple bond formation is supported by experimental evidence that increased ligand density both rescues the diffusion defect and abolishes the shear threshold (15). The diffusion defect can also be rescued by anchoring of cell-free tail mutants of L-selectin to surfaces, allowing them to interact with leukocytes expressing L-selectin ligands (14).

On all ligands tested, the tail-truncated and more so the tail-deleted L-selectin mutants support considerably shorter tethers, consistent with a role for anchorage in these local stabilization events. One possible explanation is that cytoskeletal anchorage prevents uprooting of L-selectin from the cell. However, uprooting from the plasma membrane of neutrophils has been shown to take place on the time scale of seconds (28). The tail-truncated L-selectin mutant still has two charged residues in the tail, which makes it impossible to extract it from the membrane in milliseconds. Receptor uprooting from the cytoskeleton only should lead to microvillus extension, which, however, is a slow process and has been shown to stabilize the longer-lived P-selectin-mediated rather than L-selectin-mediated tethers (29). Here we postulated another possibility for cytoskeletal regulation, namely restriction of lateral mobility. It has been argued before for integrin-mediated adhesion that increased receptor mobility due to unbinding from the cytoskeletal is used to up-regulate cell adhesion (20, 21). Indeed, increased receptor mobility is favorable for contact formation, but here we show that it is unfavorable for contact maintenance, because it reduces the probability for rebinding.

Our analysis suggests that the smallest functional tethers are mediated by a least two L-selectin bonds, each on a different microvillus, working cooperatively as one small cluster. Our model does not explain from which configuration a broken bond rebinds, but it suggests that this configuration is neither collapsed (otherwise rebinding, which implies spatial proximity, was not possible) nor strongly occupied (otherwise diffusive escape was not possible). We can only speculate that complete rupture is a multistage process, and that the rebinding discussed here starts from some partially ruptured state. We also cannot exclude that the rebinding events described here involve different partners than the dissociated ones, because both L-selectins and their carbohydrate ligands might be organized in a dimeric way. Moreover, cytoplasmic anchorage might proceed in multiple steps, including some weak preligand-binding anchorage, which is strengthened by L-selectin occupancy with ligand. Coupling between ligand binding and cytoplasmic anchorage is well known for integrins (30) and might also be at work with selectins.

The mechanisms discussed in this paper could be effective also with other vascular counterreceptors specialized to operate under shear flow. As argued here, the exceptional capacity of L-selectin to promote functional adhesion in shear flow might not result only from fast dissociation and high strength under loading, but more so from a fast rebinding rate. Indeed, other vascular adhesion receptors specialized to capture cells share on-rates similar to that of L-selectin (31). Shear flow may also promote multicontact formation for shear-promoted platelet tethering to von Willebrand factor (32). It may also enhance formation of multivalent $\alpha_4\beta_7$ and LFA-1 integrin tethers to their respective ligands (33, 34). The importance of cytoskeletal anchorage in local rebinding processes of these and related adhesion receptors has not been experimentally demonstrated to date. However, the lesson drawn here from the role of L-selectin anchorage in millisecond tether stabilization may apply to these receptors as well.

Future studies may help to confirm this hypothesis. They may also shed light on the specialized structural features acquired by these receptors and their ligands through evolution, allowing them to operate under the versatile conditions of vascular shear flow.

We thank Oren Dwir, Thorsten Erdmann, Evan Evans, Stefan Klumpp, Rudolf Merkel, Samuel Safran, and Udo Seifert for helpful discussions. R.A. is the incumbent of the Tauro Career Development Chair in Biomedical Research. U.S.S. is supported by the German Science Foundation through the Emmy Noether Program.

1. Springer, T. A. (1994) *Cell* **76,** 301–314.
2. Alon, R., Hammer, D. A. & Springer, T. A. (1995) *Nature* **374,** 539–542.
3. Alon, R., Chen, S., Puri, K. D., Finger, E. B. & Springer, T. A. (1997) *J. Cell Biol.* **138,** 1169–1180.
4. Chen, S. & Springer, T. A. (1999) *J. Cell Biol.* **144,** 185–200.
5. Chang, K.-C., Tees, D. F. J. & Hammer, D. A. (2000) *Proc. Natl. Acad. Sci. USA* **97,** 11262–11267.
6. Finger, E. B., Puri, K. D., Alon, R., Lawrence, M. B., vonAndrian, U. H. & Springer, T. A. (1996) *Nature* **379,** 266–269.
7. Alon, R., Chen, S., Fuhlbrigge, R., Puri, K. D. & Springer, T. A. (1998) *Proc. Natl. Acad. Sci. USA* **95,** 11631–11636.
8. Greenberg, A. W., Brunk, D. K. & Hammer, D. A. (2000) *Biophys. J.* **79,** 2391–2402.
9. Kansas, G. S. (1996) *Blood* **88,** 3259–3287.
10. Bell, G. I. (1978) *Science* **200,** 618–627.
11. Chen, S. & Springer, T. A. (2001) *Proc. Natl. Acad. Sci. USA* **98,** 950–955.
12. Evans, E., Leung, A., Hammer, D. & Simon, S. (2001) *Proc. Natl. Acad. Sci. USA* **98,** 3784–3789.
13. Evans, E. & Ritchie, K. (1997) *Biophys. J.* **72,** 1541–1555.
14. Dwir, O., Kansas, G. S. & Alon, R. (2001) *J. Cell Biol.* **155,** 1–13.
15. Dwir, O., Solomon, A., Mangan, S., Kansas, G. S., Schwarz, U. S. & Alon, R. (2003) *J. Cell Biol.* **163,** 649–659.
16. Goldmann, A. J., Cox, R. G. & Brenner, H. (1967) *Chem. Eng. Sci.* **22,** 653–660.
17. Tees, D. F. J., Woodward, J. T. & Hammer, D. A. (2001) *J. Chem. Phys.* **114,** 7483–7496.
18. Shoup, D. & Szabo, A. (1982) *Biophys. J.* **40,** 33–39.
19. Pavalko, F. M., Walker, D. M., Graham, L., Goheen, M., Doerschuk, C. M. & Kansas, G. S. (1995) *J. Cell Biol.* **129,** 1155–1164.
20. Chan, P. Y., Lawrence, M. B., Dustin, M. L., Ferguson, L. M., Golan, D. E. & Springer, T. A. (1991) *J. Cell Biol.* **115,** 245–255.
21. Kucik, D. F., Dustin, M. L., Miller, J. M. & Brown, E. J. (1996) *J. Clin. Invest.* **97,** 2139–2144.
22. Erdmann, T. & Schwarz, U. S. (2004) *Phys. Rev. Lett.* **92,** 108102.
23. Nicholson, M. W., Barclay, A. N., Singer, M. S., Rosen, S. D. & van derMerwe, P. A. (1998) *J. Biol. Chem.* **273,** 763–770.
24. Nguyen-Duong, M., Koch, K. W. & Merkel, R. (2003) *Europhys. Lett.* **61,** 845–851.
25. Chang, K.-C. & Hammer, D. A. (1999) *Biophys. J.* **76,** 1280–1292.
26. Marshall, B. T., Long, M., Piper, J. W., Yago, T., McEver, R. P. & Zhu, C. (2003) *Nature* **423,** 190–193.
27. Sarangapani, K. K., Yago, T., Klopocki, A. K., Lawrence, M. B., Fieger, C. B., Rosen, S. D., McEver, R. P. & Zhu, C. (2004) *J. Biol. Chem.* **279,** 2291–2298.
28. Shao, J.-Y. & Hochmuth, R. M. (1999) *Biophys. J.* **77,** 587–596.
29. Yago, T., Leppänen, A., Qiu, H., Marcus, W. D., Nollert, M. U., Zhu, C., Cummings, R. D. & McEver, R. P. (2002) *J. Cell Biol.* **158,** 787–799.
30. Hynes, R. O. (2002) *Cell* **110,** 673–687.
31. van derMerwe, P. A. & Davis, S. J. (2003) *Annu. Rev. Immunol.* **21,** 659–684.
32. Doggett, T. A., Girdhar, G., Lawshe, A., Schmidtke, D. W., Laurenzi, I. J., Diamond, S. L. & Diacovo, T. G. (2002) *Biophys. J.* **83,** 194–205.
33. deChateau, M., Chen, S., Salas, A. & Springer, T. A. (2001) *Biochemistry* **40,** 13972–13979.
34. Salas, A., Shimaoka, M., Chen, S., Carman, C. V. & Springer, T. (2002) *J. Biol. Chem.* **277,** 50255–50262.